RSC Advances

PAPER

View Article Online
View Journal | View Issue

Cite this: *RSC Adv.*, 2020, **10**, 39295

Hydrothermal synthesis of cotton-based $BiVO_4$/Ag composite for photocatalytic degradation of C.I. Reactive Black 5†

Jiangang Qu, ‡[a] Jiaqi Qian,‡[a] Mengtao Wu,[a] Qinghui Mao*[a] and Min Li *[b]

Received 4th September 2020
Accepted 19th October 2020

DOI: 10.1039/d0ra07588d

rsc.li/rsc-advances

Photocatalytic materials with high efficiency and convenient recyclability have attracted great interest for the treatment of printing and dyeing wastewater. In this paper, a narrow band gap $BiVO_4$ photocatalyst was loaded onto Ag modified cotton fabric by a hydrothermal method. The prepared composite materials were characterized by scanning electron microscopy with energy dispersive X-ray spectroscopy (SEM-EDS), X-ray diffraction (XRD), X-ray photoelectron spectroscopy (XPS) and ultraviolet visible light absorption spectroscopy (UV-vis). The composite materials as prepared show superb photocatalytic activity and reusable performance for the degradation of C.I. Reactive Black 5 (RB5). The degradation rate can reach 99% within 90 min under 1 kW xenon lamp irradiation, and over 90% of the photocatalytic performance is preserved even after five recycles. Furthermore, the photocatalytic mechanism was proposed by spectral analysis and free radical trapping experiments.

1. Introduction

Nowadays, photocatalytic technology is favored for its high efficiency, low energy consumption and wide application range.[1,2] Fujishima found that oxygen and hydrogen can be obtained by electrolyzing water with a TiO_2 electrode, marking the beginning of the photocatalytic era.[3,4] Nevertheless, the band gap of TiO_2 (>3.2 eV) is too large, and can drive a catalytic reaction only under ultraviolet light irradiation, and is incapable of fully utilizing the visible light which accounts for 43% of sunlight.[5]

Compared with TiO_2, bismuth vanadate ($BiVO_4$) has a narrow band gap of about 2.4–2.6 eV, and can absorb visible light from 400 nm to 700 nm, showing a better response to visible light. It is also non-toxic and low cost.[6] Therefore, a variety configurations of $BiVO_4$ such as microparticles,[7] microspheres,[8] microtubes[9] were prepared. However, pure $BiVO_4$ photocatalyst has a very high recombination probability of photogenerated electron hole, which leads to its low quantum efficiency. In order to improve the pollutant degradation ability, $BiVO_4$ can be modified. For example, Ag/$BiVO_4$,[10] Cu/$BiVO_4$,[11] AgI/$BiVO_4$,[12] $BiFeO_3$/$BiVO_4$,[13] RGO/$BiVO_4$,[14] $Bi_{12}TiO_{20}$/$BiVO_4$,[15] Ag@$AgVO_3$/$BiVO_4$ [16] and PDA/g-C_3N_4/$BiVO_4$ [17] ternary systems and binary systems have been reported. Nevertheless, the modified $BiVO_4$ has some disadvantages, such as small specific surface area, poor adsorption capacity and easy precipitation.

In order to solve the above problems, modified fiber-based $BiVO_4$ photocatalytic materials can be prepared, which can not only improve the degradation efficiency, but also be reused. Cotton fabric, which has large specific surface area and superior flexibility, can be processed and molded easily. In addition, the pure cotton fabric has no adsorption or degradation effect under visible light irradiation.[18] Photocatalyst particles can be deposited on cotton fabric to offer photocatalysis effect, but they are easy to fall off, which will cause secondary pollution. To strengthen the interaction between cotton fabrics and photocatalyst particles, some researchers modified the cotton surface to increase active groups. For example, J. H. Ran *et al.* loaded CuO modified $BiVO_4$ onto PDA-templated cotton, resulting in high degradation rate (97.7% after 200 min).[19] H. S. Zhang *et al.* modified $BiVO_4$ by Fe and connected with cotton fabric to prepare composite photocatalytic material with the 98.4% removal rate of Cr(VI) after 90 min.[20] Compared with Cu and Fe, Ag has better electrical conductivity. Ag nanoparticles also have the local surface plasmon resonance (SPR) phenomenon, which can enhance the absorption of visible light.[21,22]

In this study, cotton fabrics were modified with silane coupling agent KH-560 and were then loaded with Ag nanoparticles, resulting in certain conductivity and antibacterial property (Fig. S1, ESI†). Afterwards, $BiVO_4$ was uniformly loaded

[a]*School of Textile and Clothing, Nantong University, Nantong, Jiangsu 226019, China. E-mail: 1731mqh@ntu.edu.cn*

[b]*Key Laboratory of Eco-textiles, Ministry of Education, Jiangnan University, Wuxi, Jiangsu, 224122, China. E-mail: minmin0421@163.com*

† Electronic supplementary information (ESI) available: Electrical conductivity and antibacterial property of composite materials; structural formula of RB5; effects of preparation pH value and temperature on photodegradation efficiency; the FTIR spectra of composite materials; SEM images of $BiVO_4$/Ag/cotton-K; comparison of fabric strength. See DOI: 10.1039/d0ra07588d

‡ These authors contributed equally to this work and should be considered co-first authors.

on the modified cotton fabric by stirring hydrothermal method. The photocatalytic activities of the as prepared composite materials were studied by photodegradation of C.I. Reactive Black 5 (RB5, its structural formula is shown in Fig. S2†), which is one of the most widely-used azo dyes in printing and dyeing industry.[23]

2. Experimental

2.1 Materials

Cotton fabric (30 tex × 30 tex, 212/10 cm for warp and 212/10 cm for weft) was purchased from Nantong Haihui Co., Ltd and treated with acetone, ethanol and deionized water. Sodium metavanadate ($NaVO_3$), bismuth nitrate pentahydrate ($Bi(NO_3)_3 \cdot 5H_2O$), ethylenediamine tetraacetic acid disodium salt (EDTA-2Na), silver nitrate ($AgNO_3$), 3-glycidoxypropyltrimethoxysilane (KH-560) and trisodium citrate ($Na_3C_6H_5O_7 \cdot 2H_2O$) were purchased from Shanghai Chemical Reagent Co., Ltd, and used as received.

2.2 Preparation

0.5 g cotton fabric was dipped in 20 mL KH-560 solution (10 g L^{-1}) with pH of 10, and reacted at 70 °C for 30 min to obtain silane coupling agent modified cotton fabric (cotton-K). The cotton-K was immersed in the 0.1 mol L^{-1} $AgNO_3$ solution, heated to 100 °C, and then the $Na_3C_6H_5O_7$ solution was dropped. After 20 min of reaction, the fabric was taken out and dried to obtain the silver modified cotton fabric (Ag/cotton-K) (Fig. 1).

The Ag/cotton-K was added into the solution with pH of 7 containing $Bi(NO_3)_3$ (2.911 g), EDTA-2Na (2.500 g) and HNO_3 (10 mL), and kept for 30 min, then dropped the $NaVO_3$ (0.732 g) solution under stirring condition. The pH value was adjusted to 5, then whole solution was put into a micro reactor and reacted at 160 °C for 1 h under stirring to synthesis the $BiVO_4$/Ag/cotton-K. Finally, the product was washed with deionized water and dried. The synthesis condition of $BiVO_4$/Ag/cotton-K has been optimized as shown in Fig. S3.†

2.3 Characterization

The surface morphology and element composition of the composite materials were studied by SEM (ZEISS Gemini SEM 300, Zeiss, German) with energy dispersive X-ray spectrum. XRD patterns were obtained on a powder X-ray diffractometer (D8ADVANCE, Bruker, German). The 2θ scanning angle ranged from 10° to 80°. XPS was acquired by X-ray photoelectron spectroscopy (K-Alpha$^+$, Thermo Scientific, America) with an Al K-Alpha source at 30.0 eV. UV-vis was obtained by Ultraviolet visible spectrophotometer (UV-2600, Shimadzu, Japan).

2.4 Analysis of photocatalytic performance

The spectrum of the dye at 400–800 nm was determined by UV-vis spectrophotometry every 15 minutes. 50 mL RB5 dye solution (20 mg L^{-1}) was degraded by $BiVO_4$/Ag/cotton-K under the

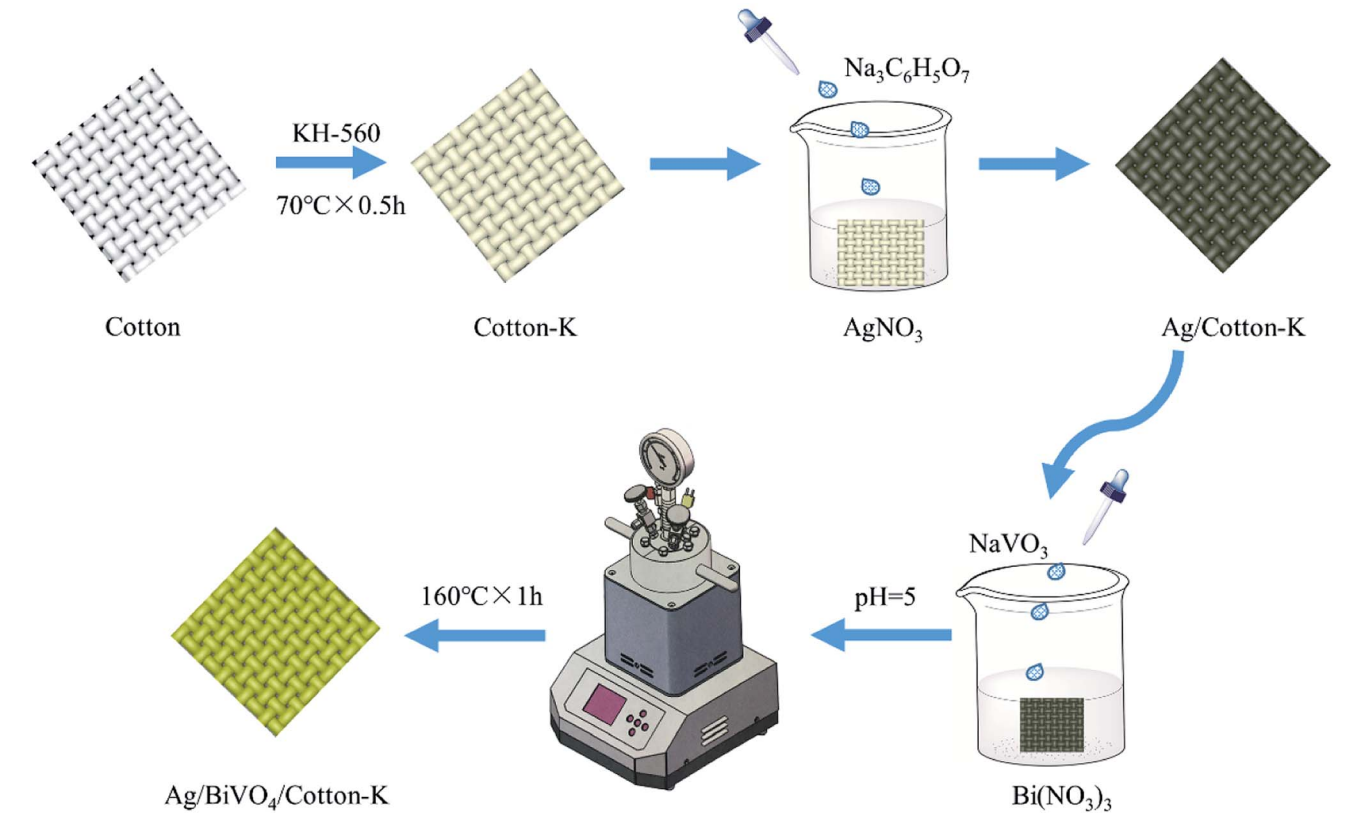

Fig. 1 Schematic diagram of the preparation process of $BiVO_4$/Ag/cotton-K.

irradiation of 1 kW xenon lamp for 90 min. The absorbance at maximum wavelength 598 nm was recorded every 15 minutes to measure its concentration. The RB5 photocatalytic degradation efficiency was obtained according to the following equation:

$$D = \frac{C_0 - C_1}{C_0} \times 100\% = \frac{A_0 - A_1}{A_0} \times 100\%$$

where C_0 and C_1 correspond to the initial and current concentrations of RB5 dye solution, and A_0 and A_1 are the initial and current absorbance of RB5 dye solution at 598 nm, respectively.

After photodegradation test, the $BiVO_4$/Ag/cotton-K was washed in deionized water and dried for recycle. Repeated dye degradation experiments were performed under the same condition as described above.

3. Results and discussion

3.1 Structure and morphology

The morphologies of cotton-K, Ag/cotton-K and $BiVO_4$/Ag/cotton-K were studied by SEM and EDS. As shown in Fig. 2a, an obvious layer of material can be seen on the surface of cotton fiber, which demonstrates that the cotton has been modified by silane coupling agent KH-560 (their FTIR spectra are shown in Fig. S4†). Ag nanoparticles and KH-560 are distributed uniformly on the fabric surface (Fig. 2b), and color of the fabric changes from white to dark green. Thanks to KH-560's cross-linking, Ag nanoparticles can be well fixed on the surface of cotton fabric. Fig. 2c and d show the morphology of $BiVO_4$/Ag/cotton-K in different magnifications (more images are shown in Fig. S5†). Monoclinic $BiVO_4$ and Ag nanoparticles are evenly distributed on the fiber surface and the fabric color turns yellow (inset in Fig. 2c).[24] In Fig. 2d, there are still a lot of Ag nanoparticles in the surface of fibers after hydrothermal synthesis. Due to the swelling of cotton fiber in the process of hydrothermal synthesis, some Ag nanoparticles have been diffused into the interface of cotton fiber, which will make Ag nanoparticles more stable. Besides, in the interface of cotton fiber, the Ag nanoparticles are in contact with $BiVO_4$ particles. The elements of the $BiVO_4$/Ag/cotton-K sample were also measured by EDS spectrum and element mapping. Six elements, including Bi, V, C, O, Si and Ag, are present and scattered distinctively on $BiVO_4$/Ag/cotton-K (Fig. 2e and f).[25] There are obvious Bi and V signals at the position of $BiVO_4$ on the fiber. Mapping images of O and Si show that both of O and Si are uniformly distributed on cotton. Due to the presence of $BiVO_4$ particles on the surface of Ag/cotton-K, there is the shadow in the mapping images of C and Ag.

3.2 XRD analysis

The phase compositions of prepared composite materials were studied by XRD, which are shown in Fig. 3a. There are four obvious diffraction peaks of cotton-K appeared at $2\theta = 14.9^\circ$, 16.7°, 23.1° and 34.6°, which are attributed to the crystallographic plane (1–10), (110), (200) and (004) of cotton fabric (JCPDS file no. 3-0226),[26] respectively. However, the characteristic peaks of Ag/cotton-K and $BiVO_4$/Ag/cotton-K at 14.9°, 16.7° and 34.6° are disappeared, and the other peak strength at 23.1° decreases obviously, indicating good combination between $BiVO_4$ and Ag with cotton. Expect for the diffraction peaks of cotton fabrics, the XRD pattern of Ag/cotton-K has extra peaks at $2\theta = 38.6^\circ$, 44.9°, 64.8° and 77.9°, which are assigned to the (111), (200), (220) and (311) crystallographic plane of Ag (JCPDS file no. 65-2871),[27] respectively. In the pattern of $BiVO_4$/Ag/cotton-K, the presence of the Ag and cotton peaks are also found. The peaks of $BiVO_4$/Ag/cotton-K are 19.4°, 29.5°, 31.1°, 35.1°, 31.8°, 40.5°, 43.0°, 46.8°, 47.4°, 47.8°, 50.8°, 53.8°, 59.0° and 60.1°, which are labeled by (110), (121), (040), (200), (002), (211), (150), (132), (240), (042), (202), (161), (321), (123) planes of the crystal faces of monoclinic scheelite type $BiVO_4$ (JCPDS file no. 14-0688).[19]

3.3 Surface elemental composition analysis

Fig. 3b–h show the elemental compositions of cotton-K, Ag/cotton-K and $BiVO_4$/Ag/cotton-K. Fig. 3b displays that the cotton-K consists of three elements, C, O and Si. In addition to these elements, the Ag/cotton-K also contains Ag element, indicating the successful loading of Ag on cotton-K. The XPS characterization reveals that $BiVO_4$/Ag/cotton-K is composed of C, O, S, Ag, Bi and V, and the conclusions are consistent with EDS, indicating that $BiVO_4$ is successfully grown on Ag/cotton-K.

As seen in Fig. 3c, the splitting peaks at binding energies of 158.6 eV and 163.9 eV, which belong to the Bi $4f_{7/2}$ and Bi $4f_{5/2}$, are the split signal of Bi 4f of Bi^{3+}.[28,29] In Fig. 3d, binding energies peaks at 516.1 eV and 523.7 eV are for V $4f_{3/2}$ and V $4f_{1/2}$, respectively, corresponding to the V^{5+} peaks of monoclinic $BiVO_4$.[29] The high-resolution spectrum of Ag 3d in Fig. 3e performs the peaks at the 367.1 eV and 373.1 eV binding energy position for Ag $3d_{5/2}$ and Ag $3d_{3/2}$, respectively, indicating the existence of Ag 3d element in the composite catalyst.[30] From Fig. 3f, the peak at 102.2 eV for Si 2p suggests the existence of Si.[31] In Fig. 3h, the peak in C 1s spectrum is divided into 284.1 eV, 285.9 eV, 287.4 eV. The peak at 284.1 eV is assigned to C–C, and the peaks at 285.9 eV and 287.4 eV are expected to C–O and C=O, respectively.[22] Fig. 3h shows the O 1s spectrum, where deconvolution of the O 1s signals are assigned to Bi–O (529.6 eV), V–O (529.1.9 eV) and C=O (532.2 eV).[20,22]

3.4 Optical absorption properties

The optical absorption properties of cotton-K, Ag/cotton-K, $BiVO_4$/cotton-K and $BiVO_4$/Ag/cotton-K were studied *via* UV-vis. The absorption of cotton-K is not obvious in the range of 250–800 nm (Fig. 4a). After loading with Ag or $BiVO_4$, the absorption of cotton-K is improved. The absorption of Ag/cotton-K composite materials in the UV-vis region is higher than that of cotton-K. In addition, $BiVO_4$/cotton-K and $BiVO_4$/Ag/cotton-K both have strong optical absorption from 250 nm to 600 nm. The absorption intensity of $BiVO_4$/Ag/cotton-K is much higher than that of $BiVO_4$/cotton-K in the range of 250–800 nm. Compared with $BiVO_4$/cotton-K, the absorption of $BiVO_4$/Ag/cotton-K exhibits a red shift, indicating strong visible light response of $BiVO_4$/Ag/cotton-K. It is attributed to the intensive localized SPR effect of Ag.[22] Furthermore, the optical band gap (E_g) of composite materials can be obtained by the following equation:[32,33]

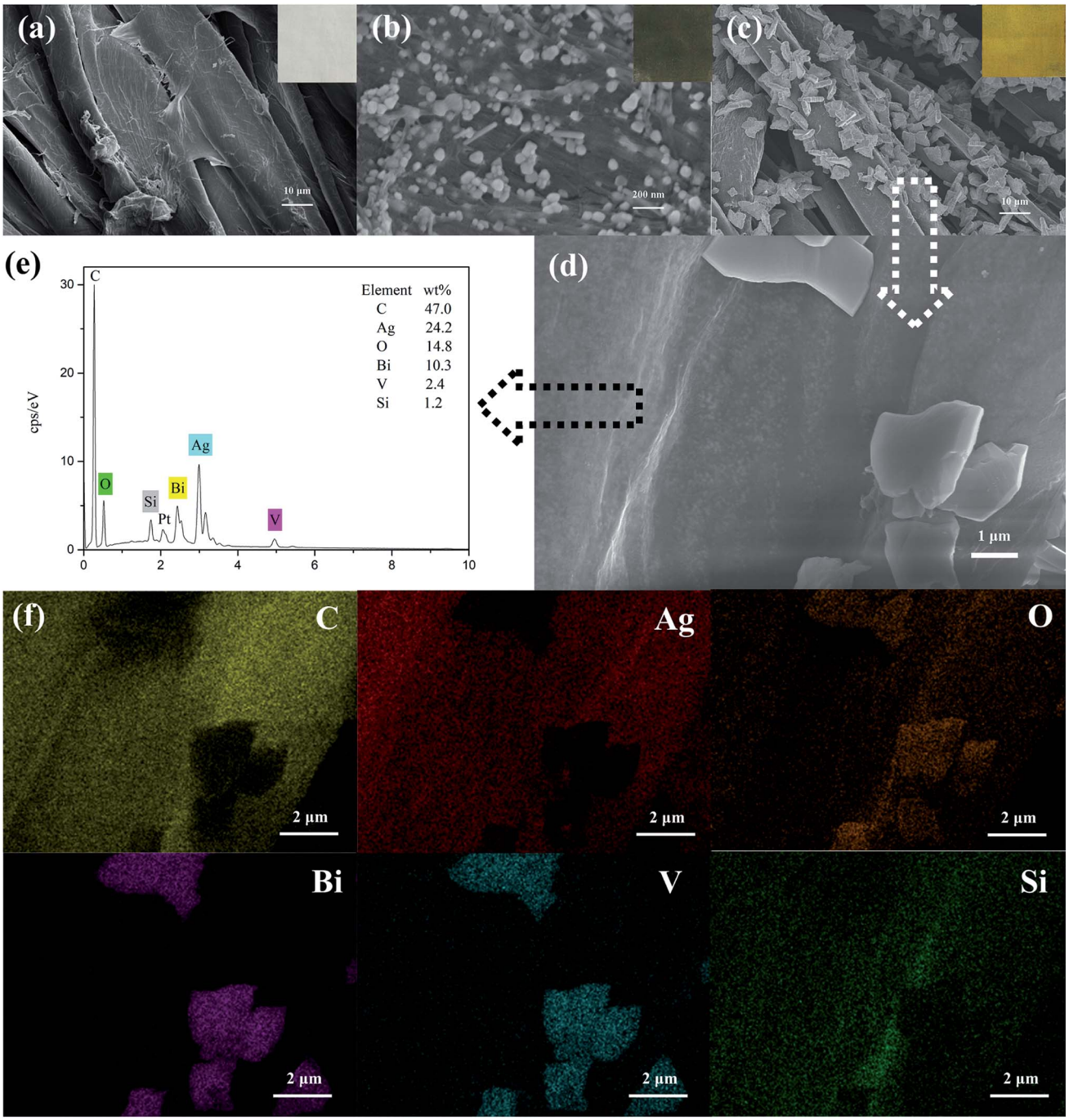

Fig. 2 SEM images of (a) cotton-K, (b) Ag/cotton-K and (c and d) $BiVO_4$/Ag/cotton-K with different magnifications. Insets are digital pictures of (a) cotton-K, (b) Ag/cotton-K and (c) $BiVO_4$/Ag/cotton-K. (e) EDS spectrum of $BiVO_4$/Ag/cotton-K in the area (d). (f) Mapping images of O, V, Ag, Si, C and Bi in the area (d).

$$(Ahv)^n = C(hv - E_g)$$

where A, v, C and E_g are the absorption coefficient, the incident light frequency, a constant and band gap, respectively. For $BiVO_4$, n is 2.[20] Therefore, according to the plots of $(Ahv)^2$ *versus* photon energy (hv) in Fig. 4b, the band gap energy of $BiVO_4$/cotton-K is 2.36 eV and that of $BiVO_4$/Ag/cotton-K is 2.29 eV. The smaller band gap implies the better photon-induced carrier separation efficiency, as well as superior photocatalytic performance.[25] The photocatalytic activity of as-prepared composite materials were evaluated by photodegradation of RB5 solution in the following part.

3.5 Photocatalytic activity and reusable performance

The degradation rate of RB5 by composite materials are shown in Fig. 5a. Under the same conditions, the absorption intensity

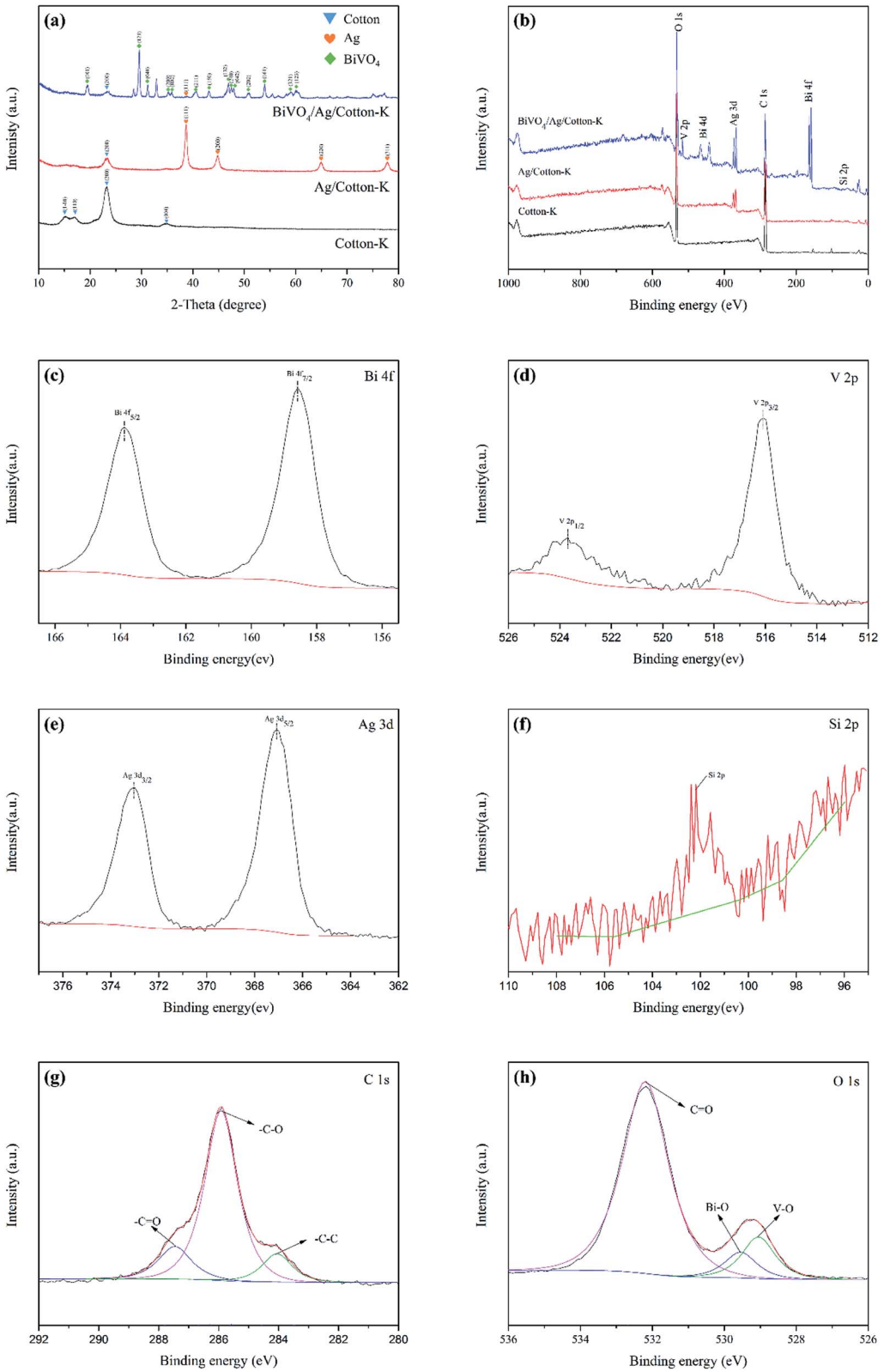

Fig. 3 (a) XRD patterns of cotton-K, Ag/cotton-K, $BiVO_4$/Ag/cotton-K. (b) XPS survey spectra. High resolution XPS spectrum of (c) Bi 4f; (d) V 2p; (e) Ag 3d; (f) Si 2p; (g) C 1s; (h) O 1s.

at 598 nm was measured every 15 minutes. The degradation rate of RB5 by $BiVO_4$/cotton-K, Ag/cotton-K and $BiVO_4$/Ag/cotton-K can reach 11%, 2% and 99% within 90 min degradation, respectively. Obviously, Ag/cotton-K has almost no photocatalytic effect, and the catalytic efficiency of Ag/cotton-K is greatly improved after loaded with photocatalyst $BiVO_4$.

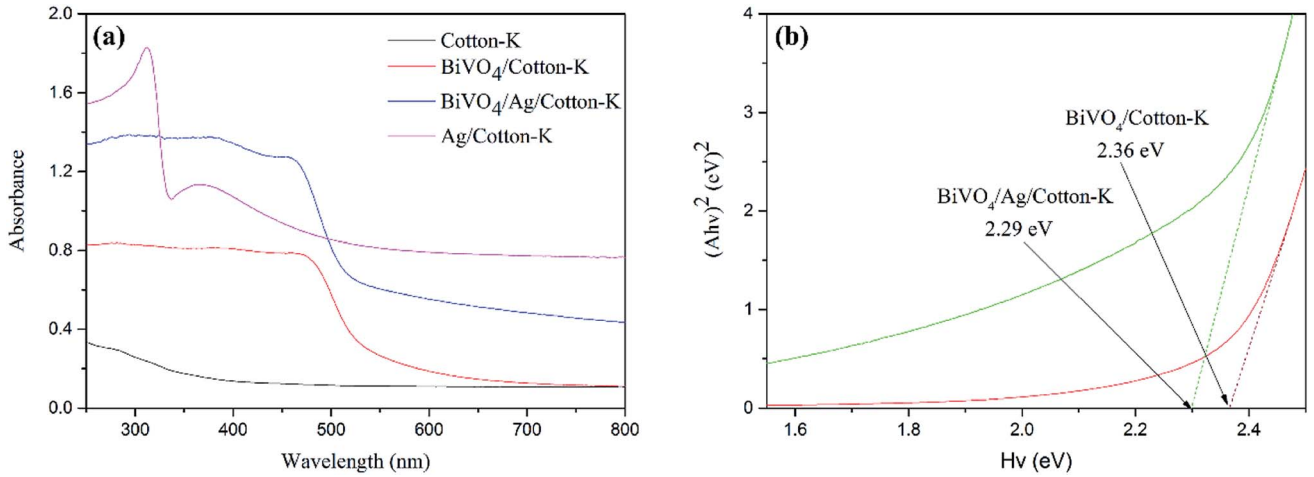

Fig. 4 (a) UV-vis diffuse reflectance spectra of all the samples and (b) band gap energy of $BiVO_4$/cotton-K and $BiVO_4$/Ag/cotton-K.

Moreover, the degradation rate of RB5 by $BiVO_4$/Ag/cotton-K is much higher than that of $BiVO_4$/cotton-K. It is due to the recombination of photo-induced charge carrier on pure $BiVO_4$ and poor conductivity of $BiVO_4$/cotton-K.[11,34] In contrast, Ag nanoparticles with good conductivity can help the electron transfer from $BiVO_4$ to the incorporated Ag nanoparticles to inhibit the recombination of holes and electrons, thus, contributing to greatly improved photocatalytic activity. The UV-vis absorption spectra of RB5 solution processed with $BiVO_4$/Ag/cotton-K were also recorded every 15 min (Fig. 5b). The UV-vis absorption peak of RB5 is at 598 nm, which gets lower and

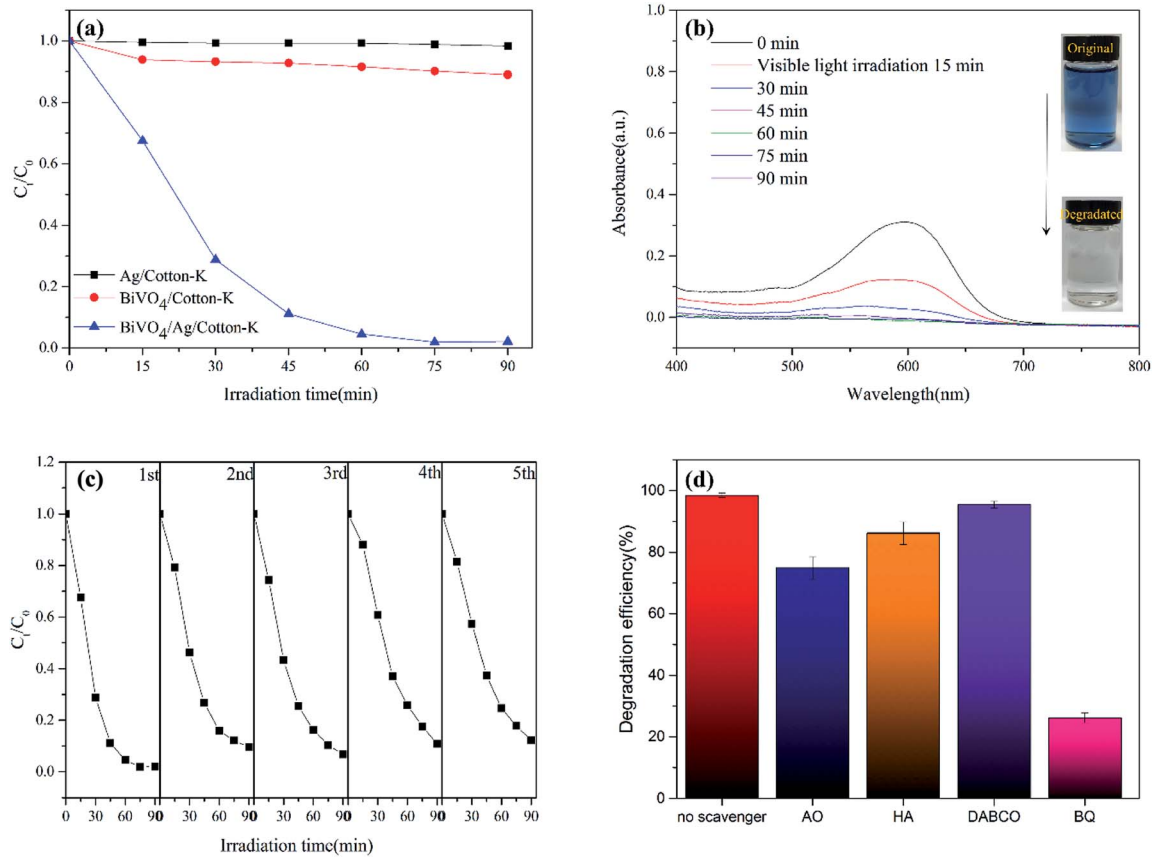

Fig. 5 (a) Photodegradation performance of RB5 under xenon light irradiation using $BiVO_4$/cotton-K, Ag/cotton-K, $BiVO_4$/Ag/cotton-K. (b) UV-vis absorption spectra of $BiVO_4$/Ag/cotton-K for the degradation of RB5 every 15 min. Insets are photos of RB5 solution before and after irradiation. (c) The recyclability of $BiVO_4$/Ag/cotton-K. (d) Trapping experiments of $BiVO_4$/Ag/cotton-K with different active species scavengers.

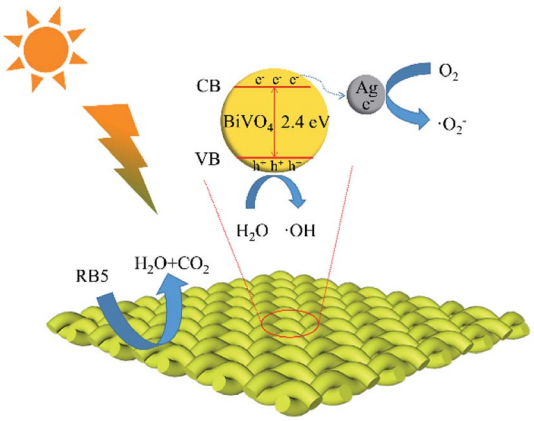

Fig. 6 Photocatalytic mechanism of $BiVO_4$/Ag/cotton-K for RB5 degradation under xenon light irradiation.

lower. After 90 min irradiation, the absorption peak disappears and the solution color completely fades.

The reusability performance of semiconductor photocatalyst is also an important indicator of the catalyst. The stability of $BiVO_4$/Ag/cotton-K was evaluated by recycling in the photodegradation of RB5 solution. After each cycle, the $BiVO_4$/Ag/cotton-K was washed and dried, and the next cycle was processed under the same condition. As shown in Fig. 5c, the degradation rate of RB5 by $BiVO_4$/Ag/cotton-K composite material is still over 90% after five cycles, and the strength decline of $BiVO_4$/Ag/cotton-K is less than that of $BiVO_4$/Ag/cotton (their warp and weft yarn strength before and after recycling five times are shown in Table S1†), demonstrating high photocatalytic activity and stability of $BiVO_4$/Ag/cotton-K.

3.6 Potential photocatalytic mechanism

The photocatalytic mechanism of $BiVO_4$/Ag/cotton-K was further studied by free radical trapping experiment. Oxalic acid (AO), benzoic acid (HA), benzoquinone (BQ), triethylenediamine (DABCO) were used to capture h^+, $^{\bullet}OH$, $^{\bullet}O_2^-$ and $^1O_2$, respectively.[20] As seen in Fig. 5d, DABCO has little effect on the degradation of RB5, which implies that $^1O_2$ has limited effect on photocatalytic reaction. In contrast, the degradation efficiency of RB5 is greatly reduced after adding scavengers AO, HA and BQ, among them, BQ has the most obvious effect. These results show that h^+, $^{\bullet}OH$ and $^{\bullet}O_2^-$ play a certain role in the degradation process, and the effect of O_2^- is the most significant.

The potential photocatalytic mechanism is proposed based on the above experimental results, as demonstrated in Fig. 6. Under light irradiation, $BiVO_4$ is excited, as well as electron (e^-) and hole (h^+) are formed on the surface of photocatalyst.[35] In the interface of cotton fiber, the Ag nanoparticles are in contact with $BiVO_4$ particles for efficient electron transfers. Thus the recombination rate of e^- and h^+ decreased with the rapid transport of e^- by Ag nanoparticles. Then h^+ reacts with H_2O and OH^- to produce $^{\bullet}OH$, and e^- reacts with O_2 to generate $^{\bullet}O_2^-$. Finally, h^+, $^{\bullet}OH$ and $^{\bullet}O_2^-$ decompose the RB5 into H_2O and CO_2. The entire sequences are summarized as follows:

$$BiVO_4 + h\nu \rightarrow BiVO_4\ (h^+ + e^-)$$

$$BiVO_4\ (e^-) + Ag \rightarrow BiVO_4 + Ag\ (e^-)$$

$$BiVO_4\ (h^+) + OH^- \rightarrow BiVO_4 + {}^{\bullet}OH$$

$$Ag\ (e^-) + O_2 \rightarrow {}^{\bullet}O_2^- + Ag$$

$$BiVO_4 + {}^{\bullet}OH + {}^{\bullet}O_2^- + RB5 \rightarrow CO_2 + H_2O$$

4. Conclusions

In conclusion, Ag modified cotton fabric supported $BiVO_4$ semiconductor photocatalyst has been successfully prepared in this work, $BiVO_4$/Ag/cotton-K shows high photocatalytic activity, and the degradation rate of RB5 reaches 99% in 90 min under xenon light irradiation. The uniform loading of Ag and $BiVO_4$ on the fabric surface has been confirmed by SEM, EDS, XRD and XPS analysis. The composite materials still have excellent reusability, and the degradation rate can reach over 90% after five cycles. It is found that h^+, $^{\bullet}OH$ and $^{\bullet}O_2^-$ participated in the photocatalytic reaction according to free radical trapping experiments.

Author contribution

Jiangang Qu, Jiaqi Qian: study design, literature research, writing-original draft, data acquisition, writing-editing, data analysis, experimental studies. Mengtao Wu: writing-review & discussion. Qinghui Mao: writing-review, data curation, project administration, validation. Min Li: resources, supervision, validation.

Conflicts of interest

The authors declare no competing financial interest.

Acknowledgements

This work was financially supported by the Open Project Program of Key Laboratory of Eco-textiles, Ministry of Education, Jiangnan University (No. KLE1708). This work was also partially supported by the National Science Foundation of China (No. 81801856), Natural Science Foundation of Jiangsu Province (No. BK20180949) and Nantong Foundation Science Research Project (No. JC2019007). The authors acknowledge the use of the Analytical Instrumentation Facility at Nantong University Analysis & Testing Center. The authors also acknowledge Dr Nanfei He from North Carolina State University for the language and writing assistance.

References

1 S. Malato, P. Fernandez-Ibanez, M. I. Maldonado, J. Blanco and W. Gernjak, Decontamination and disinfection of

water by solar photocatalysis: recent overview and trends, *Catal. Today*, 2009, **147**(1), 1–59.

2 J. Podporska-Carroll, E. Panaitescu, B. Quilty, L. L. Wang, L. Menon and S. C. Pillai, Antimicrobial properties of highly efficient photocatalytic TiO_2 nanotubes, *Appl. Catal., B*, 2015, **176**, 70–75.

3 A. Fujishima and K. Honda, Electrochemical photolysis of water at a semiconductor electrode, *Nature*, 1972, **238**(5358), 37–38.

4 A. Kudo and Y. Miseki, Heterogeneous photocatalyst materials for water splitting, *Chem. Soc. Rev.*, 2009, **38**(1), 253–278.

5 M. Ou and Q. Zhong, Ultrasound assisted synthesis of heterogeneous g-C_3N_4/$BiVO_4$ composites and their visible-light-induced photocatalytic oxidation of NO in gas phase, *J. Alloys Compd.*, 2015, **626**, 401–409.

6 A. Kudo, K. Omori and H. Kato, A novel aqueous process for preparation of crystal form-controlled and highly crystalline $BiVO_4$ powder from layered vanadates at room temperature and its photocatalytic and photophysical properties, *J. Am. Chem. Soc.*, 1999, **121**, 11459–11467.

7 F. Li, C. Y. Yang, Q. G. Li, W. Cao and T. H. Li, The pH-controlled morphology transition of $BiVO_4$ photocatalysts from microparticles to hollow microspheres, *Mater. Lett.*, 2015, **145**, 52–55.

8 A. N. Zulkifili, A. Fujiki and S. Kimijima, Flower-like $BiVO_4$ Microspheres and Their Visible Light-Driven Photocatalytic Activity, *Appl. Sci.*, 2018, **8**(2), 216.

9 L. Zhou, W. Z. Wang, L. Zhang, H. Xu and W. Zhu, Single-crystalline $BiVO_4$ microtubes with square cross-sections: microstructure, growth mechanism, and photocatalytic property, *J. Phys. Chem. C*, 2007, **111**(37), 13659–13664.

10 Z. R. Tang, Q. Yu and Y. J. Xu, Toward improving the photocatalytic activity of $BiVO_4$-graphene 2D–2D composites under visible light by the addition of mediator, *RSC Adv.*, 2014, **4**(102), 58448–58452.

11 C. Regmi, Y. K. Kshetri, R. P. Pandey, T. H. Kim, G. Gyawali and S. W. Lee, Understanding the multifunctionality in Cu-doped $BiVO_4$ semiconductor photocatalyst, *J. Environ. Sci.*, 2019, **75**, 84–97.

12 S. K. Lakhera, R. Venkataramana, G. Mathew, H. Y. Hafeez and B. Neppolian, Fabrication of high surface area AgI incorporated porous $BiVO_4$ heterojunction photocatalysts, *Mater. Sci. Semicond. Process.*, 2020, **106**, 104756.

13 B. Samran, S. Lunput, S. Tonnonchiang and S. Chaiwichian, $BiFeO_3$/$BiVO_4$ nanocomposite photocatalysts with highly enhanced T photocatalytic activity for rhodamine B degradation under visible light irradiation, *Phys. B*, 2019, **561**, 23–28.

14 T. Soltani, A. Tayyebi and B. Lee, Enhanced Photoelectrochemical (PEC) and Photocatalytic Properties of Visible-Light Reduced Graphene-Oxide/Bismuth Vanadate, *Appl. Surf. Sci.*, 2018, **448**, 465–473.

15 T. Wang, X. Y. Liu, D. L. Han, C. C. Ma, Y. Liu, P. W. Huo and Y. S. Yan, Bi-based semiconductors composites of $BiVO_4$ quantum dots decorated $Bi_{12}TiO_{20}$ via in-suit growth with ultrasound for enhancing photocatalytic performance, *J. Alloys Compd.*, 2019, **785**, 460–467.

16 P. Ju, Y. Wang, Y. Sun and D. Zhang, In situ green topotactic synthesis of a novel Z-scheme Ag@$AgVO_3$/$BiVO_4$ heterostructure with highly enhanced visible-light photocatalytic activity, *J. Colloid Interface Sci.*, 2020, **579**, 431–447.

17 R. Huo, X. L. Yang, J. Yang, S. Y. Yang and Y. H. Xu, Self-assembly synthesis of $BiVO_4$/Polydopamine/g-C_3N_4 with enhanced visible light photocatalytic performance, *Mater. Res. Bull.*, 2018, **98**, 225–230.

18 J. F. Ma, J. H. Chen, B. Wang and S. Cai, The in situ growth of $BiVO_4$ coatings on carbon fibers and their photocatalytic performance, *Mater. Res. Bull.*, 2016, **77**, 253–257.

19 J. H. Ran, H. B. Chen, X. Bai, S. G. Bi, H. Y. Jiang, G. M. Cai, D. S. Cheng and X. Wang, Immobilizing CuO/$BiVO_4$ nanocomposite on PDA-templated cotton fabric for visible light photocatalysis, antimicrobial activity and UV protection, *Appl. Surf. Sci.*, 2019, **493**, 1167–1176.

20 H. S. Zhang, D. Yu, W. Wang, P. Gao, L. S. Zhang, S. Zhong and B. J. Liu, Recyclable and highly efficient photocatalytic fabric of Fe (III)@$BiVO_4$/cotton via thiol-ene click reaction with visible-light response in water, *Adv. Powder Technol.*, 2019, **30**(12), 3182–3192.

21 N. A. Ibrahim, B. M. Eid and M. S. Abdel-Aziz, Green synthesis of AuNPs for eco-friendly functionalization of cellulosic substrates, *Appl. Surf. Sci.*, 2016, **389**, 118–125.

22 K. Ding, W. Wang, D. Yu, P. Gao and B. J. Liu, Facile formation of flexible Ag/AgCl/polydopamine/cotton fabric composite photocatalysts as an efficient visible-light photocatalysts, *Appl. Surf. Sci.*, 2018, **454**, 101–111.

23 i. A. Şengil and M. Özacar, The decolorization of C.I. Reactive Black 5 in aqueous solution by electrocoagulation using sacrificial iron electrodes, *J. Hazard. Mater.*, 2009, **161**(2–3), 1369–1376.

24 Y. L. Wang, K. Ding, R. Xu, D. Yu, W. Wang, P. Gao and B. J. Liu, Fabrication of $BiVO_4$/$BiPO_4$/GO composite photocatalytic material for the visible light-driven degradation, *J. Cleaner Prod.*, 2020, **247**, 119108.

25 L. F. Yan, B. J. Liu, W. Y. Li, T. Zhao, Y. T. Wang and Q. Q. Zhao, Multiscale cellulose based self-assembly of hierarchical structure for photocatalytic degradation of organic pollutant, *Cellulose*, 2020, **27**(9), 5241–5253.

26 D. S. Cheng, M. T. He, J. H. Ran, G. M. Cai, J. H. Wu and X. Wang, Depositing a flexible substrate of triangular silver nanoplates onto cotton fabrics for sensitive SERS detection, *Sens. Actuators, B*, 2018, **270**, 508–517.

27 R. X. Yang, F. Dong, X. You, M. Liu, S. Zhong, L. S. Zhang and B. J. Liu, Facile synthesis and characterization of interface charge transfer heterojunction of Bi_2MoO_6 modified by Ag/AgCl photosensitive material with enhanced photocatalytic activity, *Mater. Lett.*, 2019, **252**, 272–276.

28 G. Yentür and M. Dükkancl, Synthesis of Visible-Light heterostructured photocatalyst of Ag/AgCl deposited on (040) facet of monoclinic $BiVO_4$ for efficient carbamazepine photocatalytic removal, *Appl. Surf. Sci.*, 2020, **531**, 147322.

29 K. R. Tolod, S. Hernandez, M. Castellino, F. A. Deorsola, E. Davarpanah and N. Russo, Optimization of $BiVO_4$ photoelectrodes made by electrodeposition for sun-driven water oxidation, *Int. J. Hydrogen Energy*, 2020, **45**(1), 605–618.

30 L. Chen, R. Huang, Y. J. Ma, S. L. Luo, C. T. Au and S. F. Yin, Controllable synthesis of hollow and porous Ag/$BiVO_4$ composites with enhanced visible-light photocatalytic performance, *RSC Adv.*, 2013, **3**(46), 24354–24361.

31 D. Fang, X. J. Li, H. Liu, W. L. Xu, M. Jiang, W. B. Li and X. Fan, $BiVO_4$-rGO with a novel structure on steel fabric used as high-performance photocatalysts, *Sci. Rep.*, 2017, **7**, 7979.

32 S. Fakhravar, M. Farhadian and S. Tangestaninejad, Excellent performance of a novel dual Z-scheme $Cu_2S/Ag_2S/BiVO_4$ heterostructure in metronidazole degradation in batch and continuous systems: immobilization of catalytic particles on α-Al_2O_3 fiber, *Appl. Surf. Sci.*, 2020, **505**, 144599.

33 Y. H. Yan, T. J. Ni, J. G. Du, L. Li, S. Fu, K. Li and J. G. Zhou, Green synthesis of balsam pear- shaped $BiVO_4/BiPO_4$ nanocomposite for degradation of organic dye and antibiotic metronidazole, *Dalton Trans.*, 2018, **47**(17), 6089–6101.

34 P. Ju, Y. Wang, Y. Sun and D. Zhang, Controllable one-pot synthesis of a nest-like $Bi_2WO_6/BiVO_4$ composite with enhanced photocatalytic antifouling performance under visible light irradiation, *Dalton Trans.*, 2016, **45**(11), 4588–4602.

35 Y. Wang, D. Yu, W. Wang, P. Gao, L. S. Zhang, S. Zhong and B. J. Liu, The controllable synthesis of novel heterojunction CoO/$BiVO_4$ composite T catalysts for enhancing visible-light photocatalytic property, *Colloids Surf., A*, 2019, **578**, 123608.